The Breakdown of Olivine to Perovskite and Magnesiowüstite

Yanbin Wang,* Isabelle Martinez,† François Guyot,‡ Robert C. Liebermann

San Carlos olivine crystals under laboratory conditions of 26 gigapascals and 973 to 1473 kelvin (conditions typical of subducted slabs at a depth of 720 kilometers) for periods of a few minutes to 19 hours transformed to the phase assemblage of perovskite and magnesiowüstite in two stages: (i) the oxygen sublattice transformed into a cubic close-packed lattice, forming a metastable spinelloid, and (ii) at higher temperatures or longer run durations, this spinelloid broke down to perovskite and magnesiowüstite by redistributing silicon and magnesium while maintaining the general oxygen framework. The breakdown was characterized by a blocking temperature of 1000 kelvin, below which olivine remained metastable, and by rapid kinetics once the reaction was activated.

Lithospheric materials are brought into the deep mantle through subduction processes at a rate of tens of thousands of cubic kilometers per year. As the slabs descend, phase transformations occur; the kinetics and mechanisms of these transformations play a central role in controlling the mechanical properties of the slabs and have been suggested to be responsible for deep-focus earthquakes (*1*). Among the various minerals present in the subducting lithosphere, olivine is believed to be the most abundant. It is also the dominant phase in the upper mantle, and its phase transformation into the β phase is considered to be the major contributor to the seismic discontinuity at 410 km (*2*). The seismic discontinuity at 660 km is a manifestation of the disproportionation reaction of $(Mg,Fe)_2SiO_4$-spinel into perovskite and magnesiowüstite (*3*). Studies of the mechanism and kinetics of this reaction are critical to understanding the dynamics of the mantle and the fate of the subducted slabs.

We compressed San Carlos olivine crystals to 26 GPa (as found at depths of about 720 km) and heated them to temperatures between 973 and 1473 K (corresponding to the range of estimated cold and hot slab temperatures) for run durations from 0 to 19 hours (*4*). The recovered samples were examined with the use of transmission electron microscopy (TEM) (*5*).

At 973 K, olivine crystals remained metastable even after 19 hours, suggesting that this temperature is not sufficient to activate the transformation process, even under tremendous overpressure (about 14 and 10 GPa above the olivine-β and β-spinel boundaries, respectively). At 1473 K, however, a single crystal of olivine transformed in less than 30 s into a complex phase assemblage containing perovskite, magnesiowüstite, and spinel (Fig. 1). A series of experiments was then conducted at 1273 K. In 10 min, most of the sample transformed into a spinel phase. These spinel lamellae nucleated throughout the olivine crystals and formed layers of a few unit cells to about 0.1 μm (Fig. 2A). Selected-area electron diffraction (SAED) patterns indicate that the spinel is consistently oriented in the olivine, such that $(100)_\alpha \parallel (111)_\gamma$, $(010)_\alpha \parallel (2\bar{1}\bar{1})_\gamma$, and $(001)_\alpha \parallel (01\bar{1})_\gamma$, where α and γ indicate olivine and spinel, respectively. These topotactic relations agree with predictions and observations of the olivine-to-spinel transformation at lower pressures (*6*, *7*), for which a martensitic-like transformation mechanism was proposed. In this mechanism, the pseudo–hexagonal close-packed (hcp) oxygen sublattice of olivine is sheared and becomes face-centered-cubic (fcc) close-packed, and local rearrangement of the Mg and Si atoms takes place as the oxygen lattice is transformed (*8*). Some previous work suggested that the martensitic-like mechanism would operate at high levels of nonhydrostatic stress (*7*). The dislocation density in the olivine crystals varied greatly but generally was $<10^8$ cm^{-2}, suggesting a shear stress of <0.1 GPa (*9*). The transformation does not appear to be more advanced in areas of high dislocation density. Thus, our experiments confirm that in $(Mg,Fe)_2SiO_4$ olivine, the martensitic-type mechanism operates under low deviatoric stresses at 26 GPa (*10*).

The spinel lamellae are not formed within their stability field because of pressure loss during heating in the experiments. Pressure calibrations performed at 1273 K on the basis of the ilmenite-perovskite transformation in $MgSiO_3$ indicate that at this temperature, the pressure conditions of the experiments are ~2 GPa inside the stability field of perovskite + magnesiowüstite. More importantly, the amounts of perovskite and magnesiowüstite increased rapidly with time under identical pressure and temperature conditions, at the expense of spinel. Although the spinel phase dominated in the sample recovered from 1273 K after 10 min, perovskite and magnesiowüstite dominated in the 1.5-hour sample. Thus, the spinel crystals are a metastable product that represents an intermediate step in the transformation of olivine into the lower mantle two-phase mixture. The formation of metastable spinel-related phases appears to be a common phenomenon; for example, they have been observed in the β-phase stability field (*11*).

The spinel phase observed in our samples is highly disordered, and many superlattice reflections were observed (Fig. 2). In addition to strong streaking, which can be explained by stacking disorder in the spinel structure (Fig. 3A), additional reflections that are noninteger multiples of the spinel fundamentals are present (Fig. 3). Thus, the intermediate phase is not the $Fd\bar{3}m$ spinel but a related spinelloid (*11*).

In longer runs at 1273 K, the perovskite and magnesiowüstite crystals were extremely fine (0.1 μm) and typically formed narrow bands in the spinelloid matrix (Fig. 4A). The SAED patterns indicate the following topotactic relations among the three phases (Fig. 4, B and C):

$[100]_{Sp} \parallel [100]_{Mw}$, $[010]_{Sp} \parallel [010]_{Mw}$,

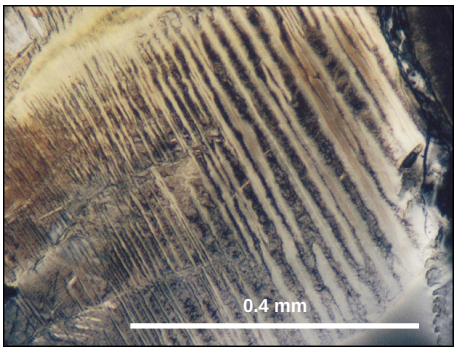

Fig. 1. Polarized optical micrograph of a single crystal of olivine recovered from 26 GPa and 1473 K. The sample was heated to the maximum temperature and quenched immediately (total time between 973 and 1473 K, about 5 min), followed by slow pressure release (40 hours). Note the pervasive lamellar features. Light lamellae are dominated by perovskite and magnesiowüstite; darker regions, metastable $(Mg,Fe)_2SiO_4$ spinelloid.

Center for High Pressure Research and Mineral Physics Institute, State University of New York, Stony Brook, NY 11794–2100, USA.

*Present address: Consortium for Advanced Radiation Sources, The University of Chicago, Chicago, IL 60637, USA.
†Present address: Laboratoire de Geochemie des Isotopes Stables and Institut de Physique du Globe de Paris, 4 place Jussieu, 75252 Paris Cedex 05, France.
‡Present address: Laboratoire de Mineralogie-Cristallographie and Institut de Physique du Globe de Paris, 4 place Jussieu, 75252 Paris Cedex 05, France.

$[001]_{Sp} \parallel [00\bar{1}]_{Mw}$ and $[100]_{Mw} \parallel [110]_{cPv}$, $[010]_{Mw} \parallel [1\bar{1}0]_{cPv}$, $[001]_{Mw} \parallel [001]_{cPv}$, where Sp, Mw, and cPv indicate spinelloid, magnesiowüstite, and cubic perovskite, respectively. The orthorhombic perovskite structure can be derived from the cubic form by continuous tilting of the SiO_6 octahedra, with the general topology remaining unchanged (*12*).

The oxygen sublattices for spinel, magnesiowüstite, and perovskite are similar (Fig. 5). For spinel, the sequence of stacking layers A, B, C, and D (about 2.05 Å between layers at zero pressure) completes one unit cell. All of these layers contain only Mg and O atoms, with a Mg population half that of O; the tetrahedrally coordinated Si atoms are halfway between these Mg-O layers. For MgO, two layers E and F form a fcc oxygen sublattice identical to that of the spinel; in these layers, the Mg and O sites are fully occupied, and the interlayer distance is about 2.10 Å at ambient conditions. The cubic perovskite has a layer G identical to the layer B in MgO (but with shorter Mg-O distances) and a layer H with much more closely packed oxygens and octahedrally coordinated Si; the interlayer distance is about 1.7 Å at zero pressure.

Our observations of the breakdown reaction may be explained by a two-step mechanism. At relatively low temperatures (below 1473 K), the hcp oxygen sublattice of olivine first transforms into a fcc arrangement with a spinelloid structure by a martensitic-like mechanism (*6*–*8*). This spinelloid then breaks down to form perovskite and magnesiowüstite. An energetically economic way for the breakdown reaction to proceed is to maintain most of the common fcc oxygen framework and to redistribute the Si and Mg atoms within the spinel lattice. As a Si^{4+} cation moves into a Mg-O layer by a small displacement of $\frac{1}{8}\langle 111\rangle_\gamma$ (arrow in layer A), the four surrounding O^{2-} anions in the layer are pulled closer together, thereby forming a part of layer H (the Si-O layer) of the perovskite. This movement causes the Mg-O bond length to increase within the layer, thus decreasing the bond strength and making it easier for the Mg^{2+} cations (M_1 and M_2 in layer A) to join the adjacent Mg-O layer (positions M_1 and M_2 in layer B) by a displacement of $\frac{1}{4}\langle 110\rangle_\gamma$. This shift doubles the Mg occupancy in layer B, making it an Mg-O layer like those in MgO and perovskite. Thus, the metastable transformation in the oxygen sublattice provides a low–activation energy path for the breakdown to proceed because little diffusion of the oxygen atoms is required.

If all the rearrangements occurred coherently while maintaining the entire topology of the oxygen framework, the result would be a structure of Mg_2SiO_4 known as the K_2NiF_4 structure, which can be viewed as being composed of alternating layers of rocksalt and perovskite (*13*). We do not have observational evidence for the existence of K_2NiF_4-structured Mg_2SiO_4, although it could be a transient and nonquenchable phase. Our model does not require formation of this phase; rather, small nuclei of perovskite and magnesiowüstite may be formed based on the fcc oxygen sublattice of the spinelloid, and then growth processes may take over. The fine-grained microstructure (Fig. 4A) supports this mechanism.

This model explains the topotactic relations among the three phases. The observed diffused satellite diffraction spots in the spinelloid may be an indication of structural disorder resulting from incomplete cation reordering after a shear mechanism affecting the oxygen sublattice. In turn, this disordering could be an additional driving force for the breakdown reaction. Experimentally, the kinetics of this reaction are

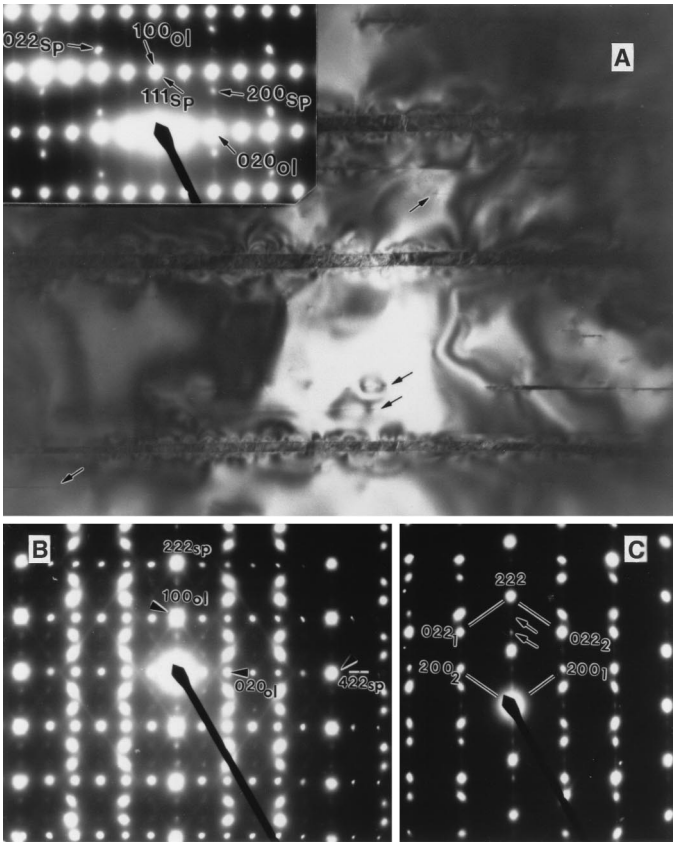

Fig. 2. Electron micrographs of a sample treated at 1273 K for 10 min. (**A**) Spinel lamellae in the olivine host, parallel to the $(100)_{ol}$ planes. Some extremely thin lamellae are indicated by arrows. Note the strain contours across the lamella interface. (**Inset**) SAED pattern indicating topotactic relations between olivine (ol) and spinel (sp). (**B**) SAED pattern taken across an interface between olivine and the spinel, showing well-defined topotactic relations between the two phases. The foil was tilted slightly from the orientation in (A). The spinel phase is heavily twinned [see (C)]; superlattice reflections and streaking indicate significant structural disorder. (**C**) SAED pattern taken within a spinel lamellae, showing pervasive {111} twinning. Spots from two crystal orientations are labeled by subscripts 1 and 2, respectively. Note also superlattice reflections in the spinel (arrows), indicating a threefold repeat along the ⟨111⟩ axes.

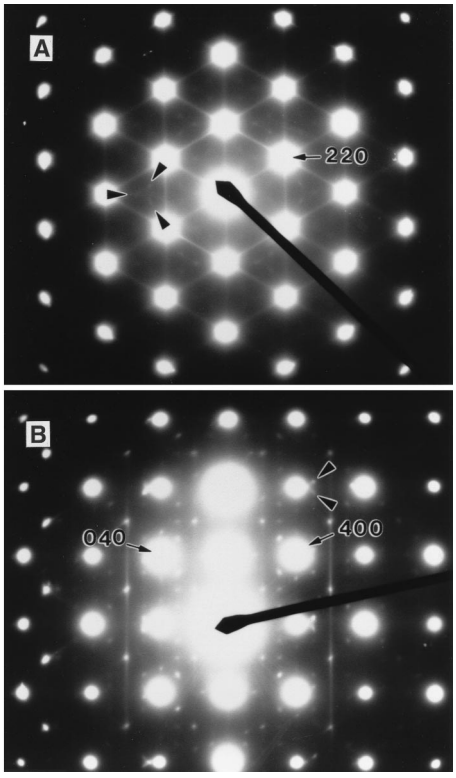

Fig. 3. SAED patterns of spinelloid indicating complex disordering and possible incommensurate behavior. (**A**) Pattern taken along the ⟨111⟩ zone axis showing streaking perpendicular to {110} resulting from the large number of stacking faults in these planes. Also notice satellite reflections (arrowheads). (**B**) The [001] zone axis. Note streaking in the vertical direction and numerous satellite reflections.

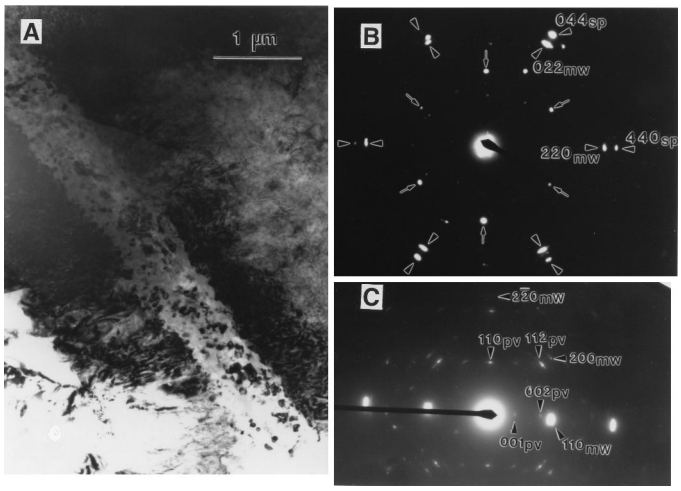

Fig. 4. (**A**) Electron micrograph showing microstructure following the breakdown reaction after 1.5 hours at 1273 K; fine-grained perovskite and magnesiowüstite form a band (upper left to lower right) within the spinelloid. Fine, dark crystals in the band are magnesiowüstite (Fe-enriched) in the perovskite (light gray, partly amorphous). (**B**) SAED pattern showing topotactic relations between spinelloid (sp) and magnesiowüstite (mw). Spinelloid spots are labeled by arrowheads pointing to the central spot; magnesiowüstite spots are labeled with arrowheads pointing outward. Notice the absence of (220) type reflections in the spinelloid and the appearance of the (⅔ ⅔ ⅔) type spots (thin arrows). (**C**) SAED pattern showing topotactic relation between perovskite (pv) and magnesiowüstite (mw).

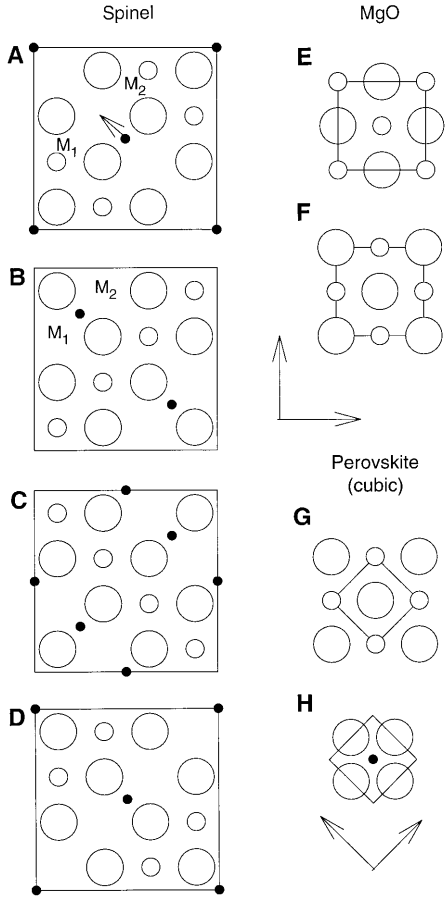

Fig. 5. Plane views of stacked layers A through H of spinel, MgO, and cubic perovskite. Large open circles represent oxygen; small open circles, Mg; and solid circles, Si atoms. All unit cell dimensions in the layers are outlined by solid lines. The third dimension is built by stacking layers on top of one another. Note that the perovskite unit cell is rotated by 45° with respect to spinel and MgO, in the same fcc oxygen framework.

extremely fast; this observation is also consistent with our model as very little diffusion is needed during nucleation of the higher pressure phase assemblage.

In subduction zones, the disproportionation reaction will weaken the slab. The breakdown reaction, originated by the martensitic-like mechanism forming the spinelloid, should reduce the shear moduli of the olivine along the slip systems that transform the hcp oxygen sublattice into a fcc arrangement (*14*), thereby weakening the slab at the transformation front. In addition, the material is composed of fine grains immediately after the transformation and may behave like a superplastic material (*15*); thus, the slab may thicken, and subduction would be inhibited. However, because the perovskite and magnesiowüstite grains coarsen rapidly at higher temperatures (*16*), the weakening of the slab is localized. Once the transformation is complete, the slab will regain its strength (now controlled only by the relatively lower temperature in the slab as compared to the surrounding mantle) and be able to continue its descent into the lower mantle.

The possible existence of a blocking temperature was recognized early on in experiments on the olivine-spinel transformations (*17*, *18*). Sung and Burns (*17*) analyzed various effects on the transformation kinetics and concluded that within the framework of the mechanisms under consideration, a blocking temperature would be expected for the Mg-rich olivine system. They suggested that the blocking temperature is essentially independent of pressure and the speed of subduction, although this conclusion has been challenged (*18*).

Our observations suggest that the concept of a blocking temperature is also applicable to the breakdown reaction to perovskite and magnesiowüstite. The fact that olivine first transforms into a spinel-related structure suggests that the temperature dependence in the breakdown kinetics is related to the blocking temperature for the olivine-spinel transformation. An additional constraint on the thermal structure of subducting slabs may thus be obtained. Global seismicity ceases at a depth of 690 km; if the phase transformations of olivine are responsible for the deep-focus earthquakes, then slab temperatures at these depths must be above the blocking temperature.

REFERENCES AND NOTES

1. S. H. Kirby, S. Stein, E. Okal, D. C. Rubie, *Rev. Geophys.* **34**, 261 (1996); S. H. Kirby, *J. Geophys. Res.* **92**, 13789 (1987); H. W. Green II and P. C. Burnley, *Nature* **341**, 733 (1989); H. W. Green II, T. E. Young, D. Walker, C. H. Scholz, *ibid.* **348**, 720 (1990); P. C. Burnley, H. W. Green, D. J. Prior, *J. Geophys. Res.* **96**, 425 (1991); H. W. Green II, T. E. Young, D. Walker, C. H. Scholz, in *High-Pressure Research: Implications in Earth and Planetary Sciences*, M. H. Manghnani and Y. Syono, Eds. (American Geophysical Union, Washington, DC, 1992), pp. 229–235.
2. See, for example, T. Katsura and E. Ito, *J. Geophys. Res.* **94**, 15663 (1989).
3. See, for example, E. Ito and E. Takahashi, in *High-Pressure Research in Mineral Physics*, M. H. Manghnani and Y. Syono, Eds. (American Geophysical Union, Washington, DC, 1987), pp. 211–229; *J. Geophys. Res.* **94**, 10637 (1989).
4. The experiments were conducted in a 2000-ton uniaxial split-sphere apparatus (USSA-2000) at the Stony Brook High Pressure Laboratory. Sample assembly and experimental techniques were described previously (*16*). In the current experiments, a mixture of coarse crystals (from 0.2 to 1.0 mm in linear dimensions) and fine powder (about 5 μm) of San Carlos olivine was used as the starting material. Microprobe analyses on the starting olivine gave an average composition of $(Mg_{0.9}Fe_{0.1})_2SiO_4$.
5. Samples were polished into standard 30-μm thin sections and then thinned by Ar ion beam. Because of the unstable nature of the silicate perovskite, a low-tension Ar beam was used (2.5 keV and 0.25 mA), and about 100 to 150 hours were required to prepare each thin foil for TEM observations. Details of the preparation techniques are described in (*16*).
6. For predictions, see J. P. Poirier, *Phys. Earth Planet. Inter.* **26**, 179 (1981); B. G. Hyde, T. J. White, M. O'Keeffe, A. W. S. Johnson, *Z. Kristallogr.* **160**, 53 (1982). For observations, see, for example, A. Lacam, M. Madon, J. P. Poirier, *Nature* **228**, 155 (1980); J. N. Boland and L. G. Liu, *ibid.* **303**, 233 (1983); M. Madon, F. Guyot, J. Peyronneau, J. P. Poirier, *Phys. Chem. Miner.* **16**, 320 (1989).
7. P. C. Burnley and H. W. Green, *Nature* **338**, 753 (1989).
8. M. Madon and J. P. Poirier, *Phys. Earth Planet. Inter.* **33**, 31 (1983).
9. See, for example, D. L. Kohlstedt, C. Goetze, W. B. Durham, in *Physics and Chemistry of Minerals and Rocks*, R. G. J. Strens, Ed. (Wiley, New York, 1976), pp. 35–49; R. C. Liebermann and Y. Wang, in *High-Pressure Research: Implications in Earth and Planetary Sciences*, M. H. Manghnani and Y. Syono, Eds. (American Geophysical Union, Washington, DC, 1992), pp. 19–31.
10. Similar observations were made by L. Kerschhofer, T. G. Sharp, and D. C. Rubie [*Science* **274**, 79 (1996)] in $(Mg,Fe)_2SiO_4$ olivine up to 20 GPa and by P. C. Burnley [*Am. Mineral.* **80**, 1293 (1995)] in the Mg_2GeO_4 system.
11. A. J. Brearley and D. C. Rubie, *Phys. Earth Planet.*

Inter. **86**, 45 (1994); Y. Wang, R. C. Liebermann, D. Cuny, L. Galoisy, *Eos* **75**, 613 (1994).
12. See, for example, Y. Wang, F. Guyot, A. Yeganeh-Haeri, R. C. Liebermann, *Science* **248**, 468 (1990).
13. R. W. G. Wyckoff, *Crystal Structures* (Interscience, New York, ed. 2, 1965), vol. 3. For earlier speculation of K_2NiF_4-structured $(Mg,Fe)_2SiO_4$, see, for example, A. E. Ringwood and A. F. Reid, *Earth Planet. Sci. Lett.* **5**, 67 (1968).
14. J. P. Poirier, in *Anelasticity in the Earth*, F. D. Stacey, M. S. Patterson, A. Nicholas, Eds. (Geodynamics Series 4, American Geophysical Union, Washington, DC, 1981), pp. 113–117.
15. D. C. Rubie, *Nature* **308**, 505 (1984); E. Ito and H. Sato, *ibid.* **351**, 140 (1991).
16. Y. Wang, F. Guyot, R. C. Liebermann, *J. Geophys. Res.* **97**, 12327 (1992); I. Martinez, Y. Wang, F. Guyot, R. C. Liebermann, J. C. Doukhan, *ibid.*, in press.
17. C.-M. Sung and R. G. Burns, *Tectonophysics* **31**, 1 (1976). Coincidentally, their rate equations predicted a blocking temperature of 973 K for the olivine-spinel transformation.
18. D. C. Rubie and C. R. Ross II, *Phys. Earth Planet. Inter.* **86**, 223 (1994).
19. The Stony Brook High Pressure Laboratory is jointly supported by the State University of New York at Stony Brook and the NSF Science and Technology Center for High Pressure Research (EAR 89-20239) and by NSF grant EAR 93-04502. Mineral Physics Institute contribution 183.

3 September 1996; accepted 21 November 1996

Transformation in Garnet from Orthorhombic Perovskite to $LiNbO_3$ Phase on Release of Pressure

Nobumasa Funamori, Takehiko Yagi, Nobuyoshi Miyajima, Kiyoshi Fujino

High-pressure in situ x-ray diffraction and transmission electron microscopy on quenched samples show that natural garnet transforms to orthorhombic perovskite (and minor coexisting phases) containing increasing amounts of aluminum with increasing pressure. This suggests that the perovskite is the dominant host mineral for aluminum in Earth's lower mantle. Orthorhombic perovskite is quenched from ~35 gigapascals but, because of the increased aluminum content, transforms to the $LiNbO_3$ structure upon quenching from ~60 gigapascals.

In 1974, Liu (*1*) reported the transformation of a natural garnet, the host mineral of Al in Earth's upper mantle, into the orthorhombic perovskite structure at 30 GPa. Since then, the transformation of garnets of various compositions has been investigated to clarify the host mineral of Al in the lower mantle. The results, however, are complicated and the host remains uncertain, whereas the hosts of the other main cations (Mg, Si, and Fe) in the mantle—$(Mg,Fe)SiO_3$ orthorhombic perovskite and (Mg,Fe)O magnesiowüstite—are well identified. Weng *et al.* (*2*) carried out experiments on pyrope ($Mg_3Al_2Si_3O_{12}$)–grossular ($Ca_3Al_2Si_3O_{12}$) garnet at 40 GPa and suggested that it transforms to an assemblage of orthorhombic perovskite and unquenchable Ca-rich perovskite. O'Neill and Jeanloz (*3*) reported the coexistence of garnet with orthorhombic perovskite up to 50 GPa in a pyrope-almandine ($Fe_3Al_2Si_3O_{12}$) system. Irifune *et al.* (*4*) found the decomposition of pyrope into a sub-aluminous (Al-deficient relative to garnet) orthorhombic perovskite and a corundum-ilmenite solid solution at pressures greater than 26.5 GPa. They also found an increase of Al in the perovskite phase with increasing pressure, and predicted the formation of an aluminous perovskite with pyrope composition above 30 to 40 GPa. Recently, Kesson *et al.* (*5*) reported that rhombohedral perovskite, rather than orthorhombic perovskite, is the stable phase of pyrope-almandine garnet at 55 to 70 GPa. On the other hand, Ahmed-Zaïd and Madon (*6*) suggested, from their experiments at 40 to 50 GPa, that the main host mineral of Al varies depending on chemical composition, pressure, and temperature. The candidates they proposed are $(Ca,Mg,Fe)Al_2Si_2O_8$ with the hollandite structure, Al_2SiO_5 with the V_3O_5 structure, and $(Ca,Mg)Al_2SiO_6$ with an unknown structure.

To clarify the host mineral of Al under lower mantle conditions, we carried out high-pressure in situ x-ray diffraction experiments on natural garnet with the use of a diamond anvil cell and synchrotron radiation (*7*). Garnet from the Udachnaya kimberlite pipe in the Sakha Republic (*8*) with the composition $Py_{49}Alm_{29}Gro_{21}Sp_1$ [Py, pyrope; Alm, almandine; Gro, grossular; Sp, spessartine ($Mn_3Al_2Si_3O_{12}$)] was ground to a powder and used as the starting material. The samples were heated by a yttrium-aluminum-garnet (YAG) laser at two different pressures (*9*). The recovered samples were examined by transmission electron microscopy (TEM) (*10*).

The sample was compressed to 67.5 GPa and heated by the YAG laser. Pressure decreased to 52.8 GPa, measured after heating. The x-ray diffraction profile (Fig. 1A) obtained after heating shows that most of the intense lines can be indexed as orthorhombic perovskite, with intensities similar to those of $MgSiO_3$ perovskite (*11*). Unit cell parameters of this phase are a = 4.539(4) Å, b = 4.761(5) Å, c = 6.622(5) Å, and V = 143.1(2) Å^3. The other lines can be assigned to Ca-rich perovskite, stishovite, and garnet. A trace amount of stishovite is often observed as a metastable phase during transformation, but it is not clear whether the stishovite observed in this sample is the metastable phase (*12*). The garnet may be a residual of the starting material that has not been heated to a high enough temperature (*9*, *13*). The orthorhombic perovskite phase was observed on decompression down to 9.6 GPa, although splitting of the characteristic triplet 020+112+200 became unclear with decreasing pressure (Fig. 1, B and C). Both a decrease of the orthorhombic distortion from cubic symmetry (*14*) and an increase of the pressure gradient across the sample during decompression can explain this phenomenon. Diffraction from the orthorhombic perovskite is not observed in the profile obtained after complete decompression (Fig. 1D). The main peaks can be indexed on the basis of rhombohedral symmetry

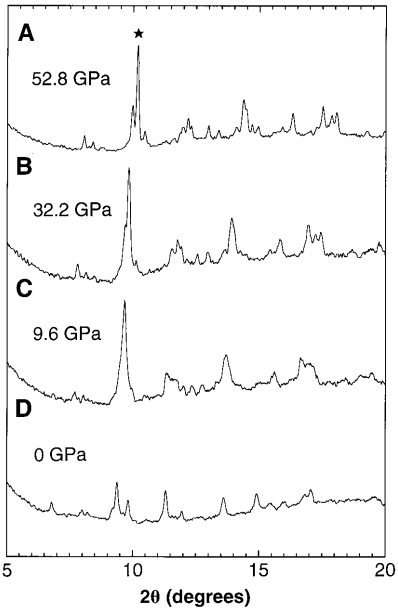

Fig. 1. X-ray diffraction profiles of the ~60 GPa sample obtained during decompression at room temperature. The star indicates the characteristic triplet 020+112+200 of orthorhombic perovskite.

N. Funamori and T. Yagi, Institute for Solid State Physics, University of Tokyo, Minato-ku 106, Japan.
N. Miyajima and K. Fujino, Department of Earth and Planetary Sciences, Hokkaido University, Sapporo 060, Japan.